Arch. Metall. Mater. **70** (2025), 2, 749-763

DOI: https://doi.org/10.24425/amm.2025.153477

Y.M. OHUNENE[1], J. OGUEGBULU[2,3], MAIA-OBI LÍGIA PASSOS[4],
F.F. MTUNZI[5], F. OJO[1], B.J. OKOLI[1,5*]

CORROSION INHIBITION OF MILD STEEL IN ACIDIC ENVIRONMENTS USING POLYPHENOL-RICH EXTRACT FROM *SENEGALIA SENEGAL* (*L.*) BRITTON STEM BARK

Corrosion presents a significant challenge to various industries, compromising the integrity and longevity of materials like mild steel. This study explores the efficacy of a polyphenol-rich fraction extracted from the stem bark of *Senegalia senegal* (PRFSS) as a green corrosion inhibitor for mild steel in acidic environments. The PRFSS extract, containing tannins, phenols, and anthocyanins, was assessed for its corrosion inhibition capabilities through various experimental methods, including gravimetric weight loss, phytochemical screening, and potentiodynamic polarization measurements. Results indicated that increasing concentrations of PRFSS notably reduced the corrosion rate of mild steel and enhanced surface coverage, suggesting effective protective layer formation. Thermodynamic analyses confirmed that the adsorption process of PRFSS onto mild steel is exothermic and spontaneous, with the adsorption behavior fitting Langmuir, Freundlich, and El-Awady isotherm models. FT-IR spectrum analysis further validated the successful adsorption of PRFSS on the mild steel surface, while TGA highlighted the extract's thermal stability. SEM images corroborated the protective role of PRFSS, showing a smoother and less corroded surface compared to untreated steel. The study demonstrates that PRFSS is a promising, environmentally benign alternative to conventional chemical inhibitors, offering significant corrosion protection for mild steel. These findings open avenues for its application in industries. Future research should investigate the long-term stability and performance of this green inhibitor under diverse operational conditions.

Keywords: Adsorption studies; Anthocyanins; Corrosion; Mild steel; Phenols; Polyphenols; *Senegalia Senegal*; Tannin, Thermodynamic studies

Introduction

Corrosion is a major threat facing industries and an understanding of preventive measures against corrosion is of high importance. It results in major loss to the integrity of materials, leading to structural failures, injuries, environmental contamination and loss of lives [1]. Mild steel, a fine ferrous metal serves as an important component of tools, equipment, devices and structures used in construction and various industries such as oil and gas, automobiles, medical, chemicals, and aviation [2]. The varied applications of mild steel in industrial processes require contact with acidic corrodent as operation agents, thus facilitating its accelerated corrosion [3]. Some consequences of mild steel corrosion include a reduced availability of industrial parts of economic and technical value, reduced value of aesthetics assets appearance, cost of maintenance and replacement of corroded industrial components, etc. [4].

The use of corrosion inhibitors have been reported as a more practical approach to address the challenges of mild steel degradation [5-8]. Corrosion inhibitors are chemical compounds which when added in small concentration to a corrosive environment, form several monomolecular layers which bars steel surfaces from acid attack, thereby decreasing or averting corrosion [9]. They may act as scavengers by weakening the corrodent in the medium or as an interface inhibitor by forming an adsorbed protective film on the mild steel surface pushing it into a passive region and halting the degradation [10].

Corrosion inhibitors that are typically synthesized from organic and inorganic chemicals usually consist of specific chemical moieties such as imidazole, urea, aldehyde, amine,

[1] BINGHAM UNIVERSITY, FACULTY OF SCIENCE AND TECHNOLOGY, DEPARTMENT OF CHEMICAL SCIENCES, PMB 005, KARU, NASARAWA STATE, NIGERIA
[2] NIGERIAN DEFENCE ACADEMY, DEPARTMENT OF CHEMISTRY, NIGERIA
[3] MEDICAL UNIVERSITY OF SOUTH CAROLINA, DEPARTMENT OF DRUG DISCOVERY AND BIOMEDICAL SCIENCES, 29425, CHARLESTON, SOUTH CAROLINA, USA
[4] FEDERAL UNIVERSITY OF ABC, CENTER OF ENGINEERING, MODELING AND APPLIED SOCIAL SCIENCES (CECS), BRAZIL
[5] VAAL UNIVERSITY OF TECHNOLOGY, INSTITUTE OF CHEMICAL AND BIOTECHNOLOGY, SOUTHERN GAUTENG SCIENCE AND TECHNOLOGY PARK, PRIVATE BAG X021, VANDERBIJLPARK 1911, SOUTH AFRICA

* Corresponding author: okolibj@binghamuni.edu.ng

ethyoxylate. Compounds of heavy metals such as lead, cadmium, arsenic, antimony, chromate, tungsten, and molybedum are also used to inhibit corrosion of iron and other metals [11]. Chemically synthesized corrosion inhibitors, however, present the shortcoming of containing heavy metals and unsafe organic moieties, some of which are generally nonbiodegradable, unrecyclable, environmentally unfriendly and toxic with hazardous effects on the ecosystem or simply expensive to synthesize [12]. Growing environmental concerns call for the replacement of chemically synthesized corrosion inhibitors with environmentally benign agents sourced from plants and other natural sources that can inhibit the corrosion of mild steel and other metals [13].

Corrosion inhibitors sourced from greener agents are considered environmentally benign, with effective corrosion inhibition ability [14]-16]. Plant-based polyphenols have been documented as having the ability to inhibit corrosion [17]. They are capable of donor-acceptor interactions using the oxygen lone pair electrons of the multiple aromatic hydroxyl groups and the metal surface [17], to form organometallic surface complexes that cling to the steel surface preventing the corrosion process [18].

A known natural source of polyphenols is the stem bark of the plant *Senegalia senegal* (*l.*) Britton commonly known as gum arabic tree and widely distributed across the dry savannah and sahel regions. It is a drought tolerant shrub naturally distributed in Northern Nigeria which has been shown to contain reasonable amounts of corrosion inhibitor agents [19,20]. Several studies, have been focused on the corrosion inhibition potentials of plant-based crude extract but none has been targeted on a specific class of phytochemical. Anand and Balasubramanian [21] investigated the corrosion behaviour of mild steel in acidic medium in presence of aqueous extract of *Allamanda blanchetii*. Studies show that various phytochemicals, including allamandin [22], tannins, flavonoids, and saponins [23] from Allamanda species, exhibit antioxidant properties beneficial for corrosion prevention. The antioxidant nature of these phytochemicals notably helps inhibit oxidative processes leading to metal corrosion [24]. Another author Garg et al. [25] evaluated the Corrosion inhibition of copper by natural occurring plant *Acacia senegal.* Similarly, phenolic compounds, flavonoids, terpenoids, and gum arabic from *A. senegal* are well-documented for their ability to form protective films over metal surfaces. Research has shown that these films effectively shield metals from corrosive elements [26,27]. Collectively, these studies support the effectiveness of phytochemicals in extracts from *A. blanchetii and A. senegal* in preventing corrosion. They emphasize mechanisms such as film formation, antioxidant activity, and metal ion complexation as means through which these compounds protect metals from corrosion.

The study demonstrated the potential of *A. senegal* extract as a green and effective corrosion inhibitor for copper in acidic environments. This finding has implications for various industrial applications where corrosion protection of copper is crucial, such as in electronics, automotive, and construction industries. This study aimed to evaluate the effectiveness of a polyphenol-rich fraction extracted from the stem bark of *S. senegal* as a corrosion inhibitor for mild steel in an acidic environment. The study investigated the influence of different temperatures and concentrations of the extract on its inhibition efficiency.

2. Methodology

2.1. Preparation of Mild Steel Test Coupons

The study employed mild steel sheets, which were transformed into test coupons measuring 2 cm × 2 cm × 0.1 cm. To achieve a smoother surface, emery paper was used to grade the surfaces. The graded test coupons were then subjected to a cleaning process using acetone to eliminate impurities. After air-drying, the cleaned test coupons were stored in a desiccator for elemental analysis and corrosion testing.

2.2. Extraction of *S. senegal* stem bark

2.2.1. Crude extraction by maceration

The stem barks of *S. senegal* were sourced from the Herbarium of the Botany section, Department of Biological Sciences, Ahmadu Bello University, Zaria, Kaduna State, with the voucher number ABU0332. The barks underwent a thorough washing process, followed by air-drying and pulverization to a particle size of 75 µm. Crude extraction was achieved through maceration, involving the complete immersion of 100 g of pulverized *S. senegal* stem bark in 200 ml of 70% acetone in a Winchester bottle. The bottle was then placed on a mechanical shaker at a temperature of 32°C for a duration of four days. The extract was separated from the acetone using a Soxhlet evaporator (349/2 Wisetherm, China) under vacuum conditions at a temperature of 40°C, as outlined in the study by Benali et al. [28]. The 30% water used in the extraction process was subsequently removed using a freeze-dryer (Cole Parmer 79203-00, USA). The resulting solid mass was stored in an airtight container for fractionation, by Solid Phase Extraction (SPE) clean-up. The percentage yield was determined using Eq. (1), which calculates the percentage of obtained extract relative to the dry weight of the stem bark.

$$Percentage\ yield = \\ = \frac{amount\ of\ tannins\ obtained\ (g)}{amount\ of\ dry\ stem\ bark\ (g)} \times 100\% \qquad (1)$$

2.2.2. Solid Phase Extraction (SPE) clean-up of the extract

To start, a 100 mg size SPE cartridge is activated using 5 mL of methanol and then 5 mL of water. Next, a polyphenol-rich fraction (dissolved in water) of 50 mL is loaded onto the cartridge. To remove impurities, the cartridge is washed with 5 mL of 5%

methanol. The elution process is done at a flow rate of 2 mL/min, using 5 mL of 80% acetonitrile. The eluates collected from this process are then concentrated using a rotary evaporator.

2.2.3. Qualitative and quantitative phytochemical screening of polyphenol fraction

Prepare a small amount of the sample polyphenol eluate and take a few drops of the eluate and transfer them to a test tube. Add 1% dilute ferric chloride solution to the test tube and observe the colour change in the solution. If polyphenols are present, a colour change will occur due to the formation of coordination complexes between the phenolic compounds and ferric ions [29].

According to a modified method based on Wadhai et al. [30], the tannin content was determined by conducting several steps. Initially, 0.5 g of the powdered polyphenol sample was weighed and transferred to a test tube. Subsequently, 10 ml of distilled water was added and thoroughly mixed. Following this, 1 ml of Folin-Ciocalteu reagent was added to the solution and mixed well. After a duration of 5 minutes, 7.5 ml of a sodium carbonate solution (20% w/v) was added. The mixture was then allowed to stand in darkness for a period of 90 minutes, during which it developed a bluish-green color. To measure the absorbance of the resulting blue color, a double beam Shimadzu Ultraviolet (UV) spectrophotometer was used at a wavelength of 750 nm. Additionally, a calibration curve was prepared utilizing a standard tannic acid solution in order to calculate the tannin content of the sample.

A portion of 0.5 g of powdered polyphenol sample was added to a test tube. To the test tube, 10 ml of distilled water was added and the contents were thoroughly mixed using a vortex mixer or shaking manually. A volume of 1 ml of Folin-Ciocalteu reagent was introduced to the test tube and mixed well with the sample. The mixture was allowed to stand at room temperature (32°C) for 5 minutes to permit color development. After the 5-minute incubation period, 7.5 ml of a 2% w/v sodium carbonate solution was added to the test tube and a thorough mixing was ensured. The test tube was then placed in a water bath set at 40°C for 90 minutes to allow the reaction to complete. After the 90-minute incubation, the test tube was removed from the water bath. The resulting blue color in the test tube was measured for absorbance at 750 nm using a double beam UV spectrophotometer. A blank solution, consisting of distilled water, Folin-Ciocalteu reagent, and sodium carbonate solution, was prepared and its absorbance was measured as a reference. A calibration curve was prepared using a standard gallic acid solution, and its absorbance at 750 nm was measured for various concentrations. The total phenolic content of the polyphenol fraction was calculated by comparing the absorbance value of the sample to the calibration curve. The total phenolic content was expressed as milligrams of gallic acid equivalents per gram (mg GAE/g) of the polyphenol sample.

According to the report, the total phenolic content was determined by first checking the color stability of the polyphenol fraction at pH 4.5. The extract was added to separate test tubes, and the pH was adjusted using a 0.1 M hydrochloric acid solution. After observing the color changes, it was determined that pH 4.5 yielded the most stable color. A citric acid-sodium citrate buffer solution at pH 4.5 was prepared. A double beam Ultraviolet (UV) spectrophotometer was used to measure the absorbance of the resulting blue color at wavelengths of 520 nm and 700 nm. These wavelengths corresponded to the absorption maxima and minima of anthocyanins, respectively. The anthocyanin content in the polyphenol fraction was calculated using the following formula based on the differences in absorbance at the two wavelengths:

$$Anthrocyanin\ content\left(\frac{\text{mg}}{\text{L}}\right)=\frac{\left(A\times MW\times DF\right)}{\left(\varepsilon\times l\right)} \qquad (2)$$

Where: A represents the absorbance difference between the two wavelengths ($\Delta A = A520\text{-}A700$), MW is the molecular weight of the anthocyanin compound, DF is the dilution factor if applicable, ε is the molar absorptivity of the specific anthocyanin compound, and l is the cuvette path length.

To determine the molar absorptivity (ε), a calibration curve was prepared using known concentrations of standard anthocyanin compounds. The absorbance of the standard solutions at both wavelengths was measured, and a graph of concentration against absorbance difference was plotted. The slope of the calibration curve represented ε.

2.3. Preparation of corrosion test media

A measured quantity of 0.2 g of the polyphenol fraction was dissolved in 1000 ml of 1M H_2SO_4 to obtain a concentration of 0.2 g/L. In addition, solutions of the polyphenol fraction were prepared at concentrations of 0.4, 0.6, and 0.8 g/L. To serve as the blank solution, an aqueous solution of 1M H_2SO_4 was prepared [31].

2.4. Gravimetric (weight loss) measurements

To measure weight loss for the purpose of weight loss, mild steel test coupons were initially weighed and then immersed individually in 50 ml of 1M H_2SO_4 in the presence and absence of a polyphenol fraction (inhibitor). The inhibitor concentrations used were 0.2, 0.4, 0.6, and 0.8 g/L, and the immersion took place in a 100 ml beaker at different temperatures of 30, 40, 50, and 60°C for a duration of 6 hours [32]. After the immersion, the mild steel test coupons were removed, dried, and weighed using an analytical weighing balance (AR2140 Adventurer, Illinois, USA). The corrosion rate (mg cm^{-2} h^{-1}), percentage inhibitor efficiency ($IE\%$), and degree surface coverage (θ) were then calculated using equations 3, 4, and 5 respectively, as described by Adejoro et al. [33]. Where; W represents the weight loss (g), T denotes the immersion time (hrs), A signifies the area of the mild steel test coupon (cm^2), W_1 indicates the weight loss of the

mild steel coupon with the inhibitor in an acidic medium (g), and W_2 is the weight loss of the mild steel coupon without the inhibitor in an acidic medium (g).

$$Corrosion\ rate = \frac{24W}{AT} \tag{3}$$

$$IE\,\% = 1 - \frac{W_1}{W_2} \times 100 \tag{4}$$

$$Degree\ surface\ coverage\ (\theta) = 1 - \frac{W_1}{W_2} \tag{5}$$

2.5. Adsorption and thermodynamic quantities

To explain the process of adsorption of polyphenol fraction (inhibitor) on the mild steel test coupon, the degree of surface coverage calculated from gravimetric studies were fitted into an empirical model of Langmuir, Freundlich and El-Awady isotherms using Eqs. 6-8 according to Adejoro et al. [33] and Aralu et al. [34]. Where: θ represents the degree of surface coverage, C denotes the inhibitor concentration, K_{ads} is the equilibrium constant for the adsorption process, $1/n$ corresponds to the slope, Log$K$ signifies the intercept, K is the isotherm constant, and y indicates the number of inhibitor molecules.

Langmuir isotherm is given as;

$$\frac{C}{\theta} = \frac{1}{K_{ads}} + C \tag{6}$$

Freundlich isotherm is given as;

$$\mathrm{Log}\theta = \mathrm{Log}K + \frac{1}{n}\mathrm{Log}C \tag{7}$$

El-Awady Isotherm is given as;

$$\mathrm{Log}\frac{\theta}{1-\theta} = \mathrm{Log}k + y\mathrm{Log}C \tag{8}$$

The thermodynamic parameters were determined according to Eqs. 9-12. Where θ represents the surface coverage degree, C is the inhibitor concentration, K_{ads} denotes the equilibrium constant of the adsorption process, R stands for the molar gas constant (8.314 kJ/mol), and T is the temperature in Kelvin. Specifically, T_1 is the temperature at 303 K, T_2 is the temperature at 323 K, θ_1 indicates the surface coverage degree at T_1, and θ_2 indicates the surface coverage degree at T_2.

Equilibrium constant of adsorption:

$$(K_{ads}) = \frac{\theta}{[(1-\theta)C]} \tag{9}$$

Gibbs free energy of adsorption (ΔG°_{ads}) is given as

$$\Delta G^{\circ}_{ads} = -2.303\ RT\ \mathrm{Log}(55.5K_{ads}) \tag{10}$$

Enthalpy of adsorption (Q_{ads}) is given as;

$$Q_{ads} = 2.303R\left[\mathrm{Log}\frac{\theta_2}{1-\theta_2} - \mathrm{Log}\frac{\theta_1}{1-\theta_1}\right] \times \frac{T_2T_1}{T_2 - T_1} \tag{11}$$

Adsorption Activation Energy (E_a) is given as;

$$\mathrm{Log}\frac{CR_2}{CR_1} = \frac{E_a}{2.303R}\left[\frac{T_2 - T_1}{T_1T_2}\right] \tag{12}$$

Where R is the molar gas constant (8.314 kJ/mol), T_1 represents temperatures 303 K, T_2 represents temperatures 323 K, CR_1 represent corrosion rate at T_1, and CR_2 represents corrosion rate at T_2.

2.6. Potentiodynamic polarization measurement

The potentiodynamic polarization measurement was conducted in a freshly prepared acidic blank solution as well as in solutions containing different concentrations (0.2, 0.4, 0.6, and 0.8 g/L) of the polyphenol fraction (inhibitor). The measurements were performed at a constant temperature of 30 ± 0.1°C using a potentiostat device (ASTM G-61, Pennsylvania, USA). The device used a 3-electrode setup consisting of a reference electrode, a counter electrode, and a working electrode. In this case, the mild steel test coupon (MSTC) under investigation served as the working electrode. The potentiodynamic current-potential curves were recorded under experimental conditions including a set potential of 2.00 V, a scan rate of 0.10 V per second, and an interval time of 0.167 seconds [35]. The values of I_{corr} obtained from the anodic and cathodic curves of the Tafel plot were used to calculate the percentage inhibitor efficiency (%IE) using equation 13 [36]:

$$IE\% = 1 - \frac{I_{corr(inh)}}{I_{corr(blk)}} \times 100 \tag{13}$$

Where $I_{corr(inh)}$ is the corrosion current density in the inhibited medium and $I_{corr(blk)}$ is the corrosion current density in the uninhibited medium.

2.7. Characterization of polyphenol fraction and mild steel test coupon

The polyphenol fraction (inhibitor) was analyzed for its functional group composition using FT-IR. The scanning was done in the range of 4000 to 400 cm^{-1} using a PerkinElmer Spectrum 400 instrument. The surface morphology of the samples was observed using a Jeol JSM-6400 emission electron microscope. The thermal properties of the composites were determined through thermal gravimetric analysis (TGA 4000). The composites were subjected to a heating rate of 10°C/min under a nitrogen flow (100 mL/min) from ambient temperature to 900°C. The mass loss and calorific changes were recorded and plotted as thermal gravimetric (TG) curve. The same procedure was followed for the mild steel samples.

3. Results and discussion

3.1. Quantitative Analysis of Polyphenol-Rich Fraction of *S. Senegal* (PRFSS)

The phytochemical screening of polyphenol fraction (inhibitor) revealed the presence of tannins, phenols, and anthocyanins. The concentration of tannins was found to be 23.81 mg/100 g, while the concentration of phenols and anthocyanins was 865.84 mg/100 g and 90.04 mg/100 g respectively (TABLE 1).

TABLE 1

Quantitative phytochemical screening of polyphenol fraction

Phytochemical Constituents	Sample Concentration (mg/100g)
Tannins	23.81
Total Phenol	865.84
Anthocyanins	90.04

The primary components of PRFSS include tannins, phenols, and anthocyanins, typically found as gallic acid, catechin, epicatechin, cyanidin-3-glucoside, cyanidin, and malvidin (Fig. 1). Gallic acid, catechin, and epicatechin possess three hydroxyl groups on their aromatic rings. Cyanidin-3-glucoside is an anthocyanin characterized by a glycosylated structure. Hydroxyl and methoxy groups facilitate multiple attachment points to metal surfaces by donating electrons.

These findings are supported by previous research, which has shown that *S. senegal* is a rich source of polyphenols. Sow [37] found that the *S. senegal* contains a variety of phenolic compounds, including gallic acid, catechin, and epicatechin.

These molecular structures provide insights into the specific mechanisms and efficacy of these compounds in inhibiting corrosion. Studies have shown that tannins, phenols, and anthocyanins can form complexes with metal ions, which can prevent corrosion co-factors from interacting with the surface of metal and causing corrosion [38-40].

3.2. FT-IR spectrum of PRFSS

The spectrum of PRFSS (Fig. 2) shows a broad peak at 3220 cm^{-1}, which is characteristic of O-H stretching vibrations of phenolic compounds and is superposing a peak at 2930 cm^{-1}, which is due to C-H aliphatic stretching vibrations.

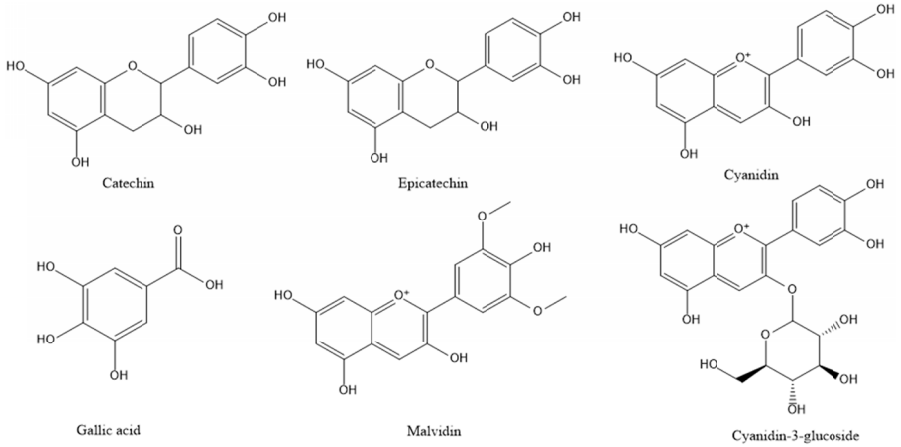

Fig. 1. Chemical structures of the major constituents of PRFSS

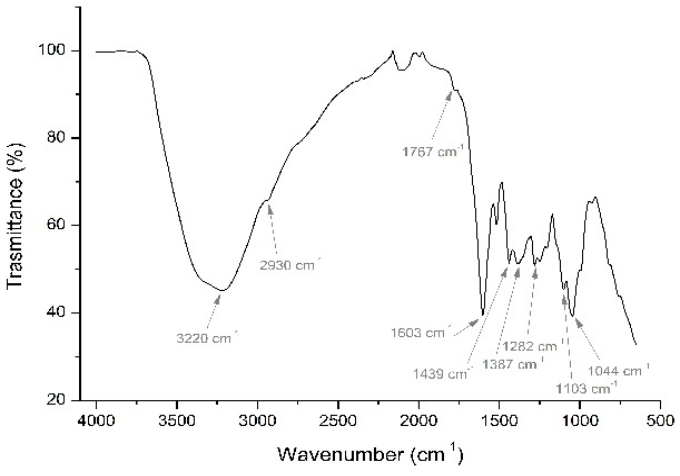

Fig. 2. FTIR spectrum of PRFSS

The peak due to the aromatic C-H stretching vibrations cannot be discerned at the spectra, but contributes to the broadening of the peak at 3209 cm^{-1}. A shoulder is seen at 1767 cm^{-1}, which can be attributed to the stretching of C=O bonds from esters groups of the tannins. The peak at 1603 cm^{-1} is due to C-C stretching vibrations in aromatic rings; the peaks at 1439 and 1387 cm^{-1} are due to C-H deformation vibrations, the peak at 1282 cm^{-1} is due to C-O-C stretching vibrations in aromatic groups and the peaks at 1103 and 1044 cm^{-1} are due to C-O stretching vibrations. These peaks evidence the presence of polyphenols in the extracts. Ndiwe et al. also studied the S. Senegal extract obtaining the same peaks at the FTIR spectra [41]. Phenols, tannins, anthocyanins and other polyphenols present aromatic rings, ether and hydroxyl groups as functional groups and, therefore, they present similar FTIR spectra [42-44]. Due to

this similarity, FTIR alone cannot be used to identify individual classes of phenols or polyphenols.

3.3. Thermal Stability of PRFSS

The TGA and DTG curves of PRFSS are shown in Fig. 3. The TGA curve shows that the extract undergoes two main stages of decomposition. The first stage occurs between 100 and 250°C, with a weight loss of about 10%. This stage is attributed to the loss of moisture from the extract. The second stage occurs between 300 and 500°C, with a weight loss of about 60%. This stage is attributed to the decomposition of the organic matter in the extract.

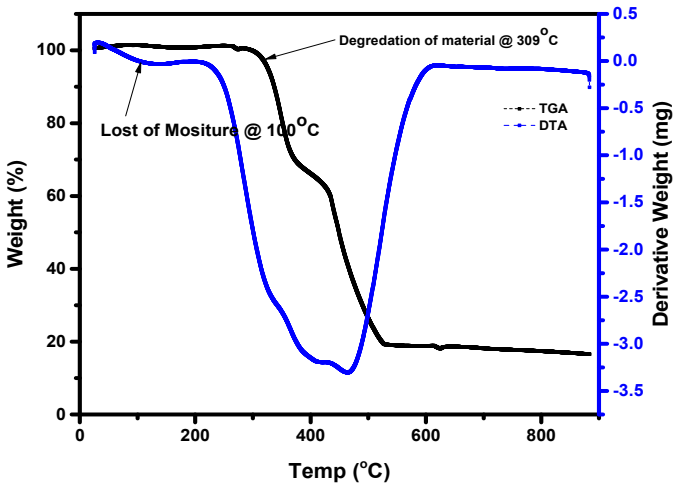

Fig. 3. TGA and DTG profiles of PRFSS

The DTG curve shows that the rate of weight loss is highest between 300 and 400°C. This indicates that the decomposition of the organic matter in the extract occurs most rapidly in this temperature range.

The TGA and DTG curves of tannin rich extract of *S. Senegal* are similar to those of other plant materials. For example, the TGA curve of tannin rich extract of *S. Senegal* is similar to that of tannin rich extract of *Acacia nilotica*, which also undergoes two main stages of decomposition. The first stage occurs between 100 and 250°C, with a weight loss of about 10%, and the second stage occurs between 300 and 500°C, with a weight loss of about 60%. The DTG curve of tannin rich extract of *S. Senegal* is also similar to that of tannin rich extract of *A. nilotica*, which shows that the rate of weight loss is highest between 300 and 400°C.

3.4. Elemental Analysis of Mild Steel Test Coupon

TABLE 2 presents the XRF analysis result, revealing the elemental composition of the mild steel Test Coupon. The results clearly demonstrate a significant presence of iron (Fe), alongside the presence of other elements including aluminium, silicon, carbon, and cobalt. According to a study by Saxena and Mishra [45], iron (Fe) is an essential element in mild steel composition, as it provides strength and durability. Aluminium is known for its ability to improve the corrosion resistance of steel [46]. Silicon is commonly used as a deoxidizer, playing a crucial role in improving the mechanical properties of steel [47]. Carbon, as an integral part of steel, determines its hardness and strength [48]. Cobalt, although present in relatively smaller quantities, can enhance the strength and high-temperature properties of steel [49]. Therefore, the XRF analysis, as presented in TABLE 2, aligns with the existing literature regarding the elemental composition of mild steel.

TABLE 2

Elemental Composition of Mild Steel Test Coupon (MSTC)

Element	Fe	C	Al	Si	Co
Composition (%)	89.04	1.89	4.41	4.16	0.29

3.5. Effect of PRFSS Concentration on Corrosion Rate and Surface Coverage of Mild Steel

The effect of increasing PRFSS concentration on corrosion rate and surface coverage of mild steel in 0.5M H_2SO_4 as temperature increases from 30-60°C is shown in Fig. 4(a-d). It can be seen that the corrosion rate decreases with increasing extract concentration. This is due to the fact that the extract contains polyphenols, which are known to be effective corrosion inhibitors. Polyphenolic compounds can form a protective layer on the metal surface, thereby preventing the metal from coming into contact with the corrosive environment. The surface coverage increases with increasing extract concentration, which further confirms the formation of a protective layer on the metal surface.

The results of this study are consistent with the study by Ebenso et al. [50] which found that *Psidium guajava* extract was an effective corrosion inhibitor for mild steel in 0.5M H_2SO_4. The study found that the corrosion rate of mild steel decreased with increasing PRFSS concentration, and that the surface coverage of mild steel increased with increasing *S. Senegal* extract concentration. The protective layer is more effective at higher concentrations of *S. Senegal* extract, which results in a higher surface coverage.

Another study by Oguzie et al. [51] found that *P. guajava* extract was effective in inhibiting the corrosion of mild steel in saline solution. The authors found that the extract was able to form a protective layer on the metal surface, which prevented the metal from coming into contact with the corrosive environment. Further, Okafor et al. [52] found that *P. guajava* extract was effective in reducing the corrosion rate of mild steel in alkaline media. The results of this study suggest that *S. Senegal* extract is a promising natural corrosion inhibitor for mild steel. The extract is effective in reducing the corrosion rate of mild steel in both acidic and alkaline media. The extract is also non-toxic and bio-

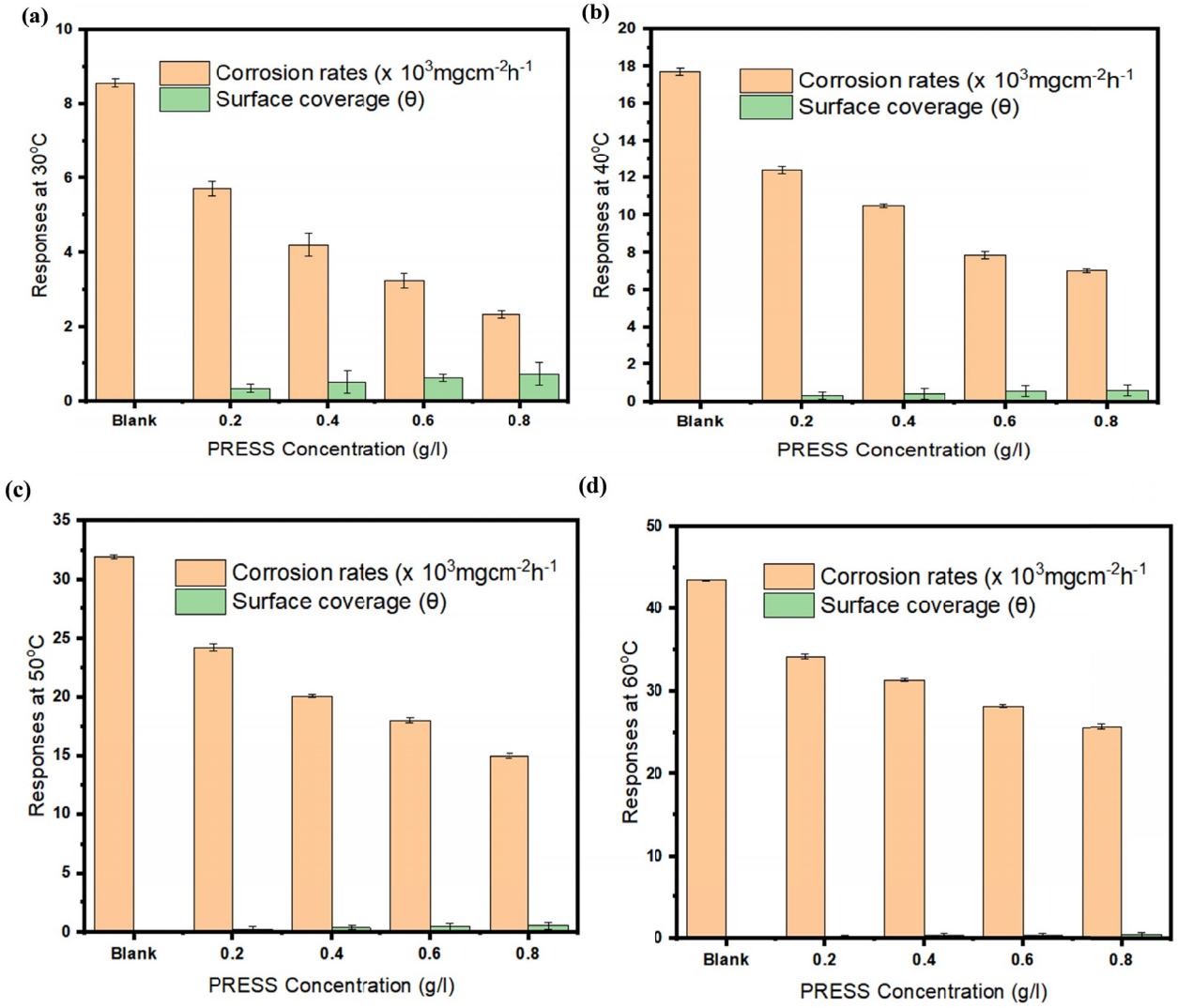

Fig. 4. Calculated values of corrosion rates and surface coverage at (a) 30°C, (b) 40°C, (c) 50°C, and (d) 60°C for mild steel corrosion in 1M H_2SO_4 and PRFSS inhibitor

degradable, making it an environmentally friendly alternative to traditional corrosion inhibitors. The study found that the extract reduced the corrosion rate by up to 90%. A reduction in corrosion rate by up to 80% in mild steel was reported for *P. guajava* extract in 0.5 M H_2SO4 solution by Umoren et al. [53].

In Fig. 4(a-d), it can be observed that the corrosion rate of mild steel in the blank solution (without PRFSS) increases with increasing temperature. This is because the increase in temperature provides more energy to overcome the energy barrier for corrosion reaction to occur, leading to a faster rate of metal dissolution. When the temperature increases by 10°C, the rate of corrosion of mild steel increases by 2.44 times between 30°C to 40°C, by 2.1 times between 40°C and 50°C, and by 1.5 times between 50°C and 60°C. On average, when the temperature increases by 10°C, the rate of corrosion of mild steel increases by 2.01 times.

This is similar to findings of Konovalova [54] on the effects of temperature on corrosion rate of iron-carbon alloys which reported a 2.3 times average increase in corrosion rate for every 10°C increase in temperature.

The addition of PRFSS to the solution decreases the corrosion rate of mild steel at all temperature points. As the concentration of PRFSS increases, the surface coverage of the metal increases, which leads to a decrease in the corrosion rate (Fig. 4(a-d)). The effect of temperature on the corrosion rate of mild steel in the presence of PRFSS is not as significant as the effect of concentration. This is because the protective layer formed by the polyphenols is able to withstand temperatures of 30°C-60°C.

3.6. Inhibition Efficiency of PRFSS Inhibitor on Mild Steel

The effect of increasing temperature and increasing PRFSS concentration on percentage corrosion inhibition efficiency (%*IE*) of mild steel in 1M H_2SO_4 (Fig. 5).

It can be seen that the percentage corrosion inhibition efficiency increases with increasing concentration of PRFSS. This is because the extract contains compounds that act as cor-

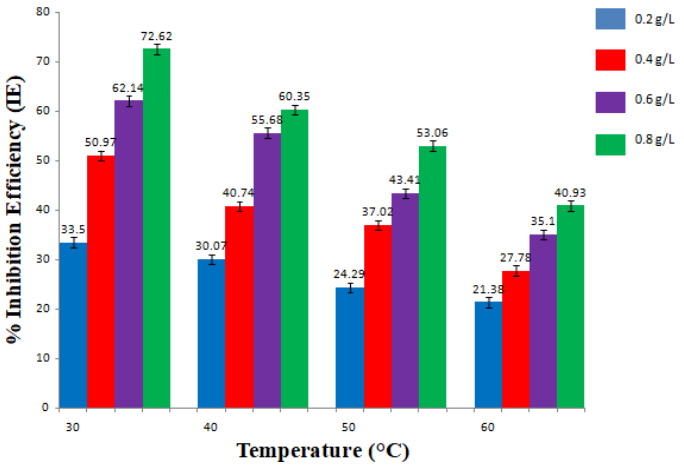

Fig. 5. Inhibition efficiency percentages of PRFSS at various concentrations on mild steel in 1M H_2SO_4 across different temperatures

rosion inhibitors, and increasing the concentration of the extract increases the amount of these inhibitors present on the surface of the metal, which results in a higher degree of protection against corrosion. The percentage corrosion inhibition efficiency also decreases with increasing temperature. This is because the increased temperature provides more energy for the corrosion reaction to occur, which overcomes the protective effect of the inhibitors.

The results of this study are consistent with those of Ebenso et al. [50] found that *P. guajava* extract inhibited the corrosion of mild steel in 1M HCl solution, and that the percentage corrosion inhibition efficiency increased with increasing concentration of the extract. According to Oguzie et al. [51], it was observed that the presence of *P. guajava* extract inhibited the corrosion of mild steel in a solution of 0.5M H_2SO_4. The study also revealed that the effectiveness of corrosion inhibition, expressed as the percentage of corrosion inhibition efficiency, was positively correlated with the concentration of the extract. On the contrary, as temperature increased, the corrosion inhibition efficiency decreased.

3.7. Adsorption and Thermodynamics Considerations

3.7.1. Langmuir adsorption model

In Fig. 6, the adsorption of PRFSS onto mild steel, the Langmuir model provides a good fit to the experimental data, with a R^2 values between 0.8969-0.9338. The maximum adsorption capacities of the mild steel surface as temperature increases from 30°C to 60°C results in increase in equilibrium constant is found to be 0.84-1.63 L/g. This indicates that the PRFSS has a strong affinity for the mild steel surface and that the adsorption process is reversible.

The model's prediction is supported by the observation that the maximum coverage and absorption coefficient increase as the temperature increases. This suggests that the process of adsorption of PRFSS onto mild steel is a physisorption process, involving weak van der Waals forces between the adsorbate and the adsorbent. Furthermore, at higher temperatures, the extract molecules are more strongly attracted to the mild steel surface.

Other studies have also found that the Langmuir adsorption model effectively describes the adsorption of *S. senegal* extract onto various metal surfaces. In the study conducted by Jouhari et al. [55], it was established that the Langmuir adsorption model is suitable for describing the adsorption of *S. senegal* extract onto copper. Similarly, another study by Jouhari et al. [56] concluded that the Langmuir adsorption model accurately represents the adsorption of *S. senegal* extract onto aluminum.

Goodness of Fit	30°C	40°C	50°C	60°C
R^2	0.8969	0.8987	0.9338	0.9110
P value	0.0145	0.0141	0.0074	0.0116
Equation	Y = 1.29*X + 0.17	Y = 1.53*X + 0.20	Y = 0.63*X + 0.06	Y = 2.33*X + 0.28

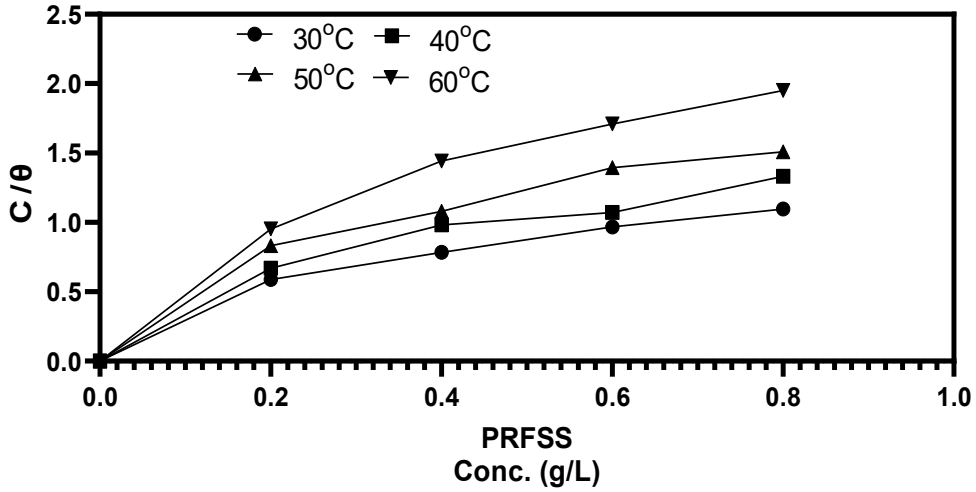

Fig. 6. Plot of Langmuir adsorption model for PRFSS inhibitor on mild steel in 1M H_2SO_4 and 0.2-0.8 g/L PRFSS inhibitor concentration at 30, 40, 50, and 60°C

3.7.2. Freundlich adsorption model

The Freundlich adsorption model of the plot of log of PRFSS concentration against logθ of mild steel shows a general increase in temperature with decrease adsorption capacity and heterogeneity of adsorbent surface (Fig. 7). In the case of the adsorption of PRFSS on mild steel, the Freundlich adsorption model was found to fit the data well, with a R^2 values between 0.9847-0.9986. The values of the Freundlich constant, K, and the Freundlich exponent, n, were found to be 0.48-0.7 and 1.79-2.08, respectively. This indicates that the adsorption of PRFSS on mild steel is a heterogeneous process and that the adsorbent has a high adsorption capacity.

3.7.3. El-Awady adsorption model

The experimental data in Fig. 8 are consistent with the predictions of the El-Awady adsorption model. The surface coverage of the mild steel by PRFSS increases with increasing PRFSS concentration and temperature. The slope of the plot of log of PRFSS concentration against log(θ/1-θ) also increases with increasing temperature.

According to El-Awady et al. [57], it was found that this adsorption model can be used to describe the adsorption of other solutes onto other solid surfaces; as described in the adsorption of methylene blue onto activated carbon. Another study by El-Khaiary et al. [58] found that the adsorption model could be used to describe the adsorption of phenol onto silica gel.

Goodness of fit	30°C	40°C	50°C	60°C
R2	0.9986	0.9847	0.991	0.9917
P value	0.0007	0.0077	0.0045	0.0041
Equation	Y = 0.5476*X - 0.08250	Y = 0.5265*X - 0.1586	Y = 0.5556*X - 0.2268	Y = 0.4833*X - 0.3481

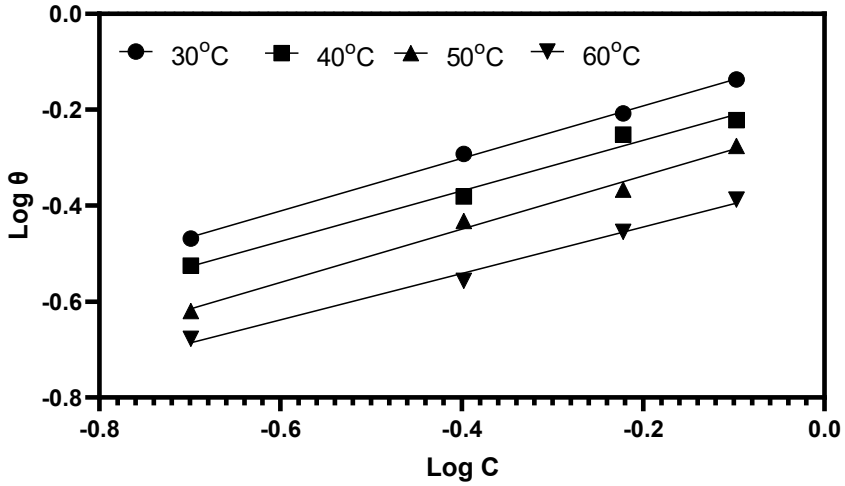

Fig. 7. Freundlich adsorption model values for mild steel in 1M H_2SO_4 and 0.2-0.8 g/L PRFSS concentration at 30, 40, 50, and 60°C

Goodness of fit	30°C	40°C	50°C	60°C
R2	0.9866	0.9708	0.9861	0.9835
P value	0.0067	0.0147	0.007	0.0083
Equation	Y = 1.163*X + 0.5049	Y = 0.9501*X + 0.2730	Y = 0.8810*X + 0.1113	Y = 0.6893*X - 0.1101

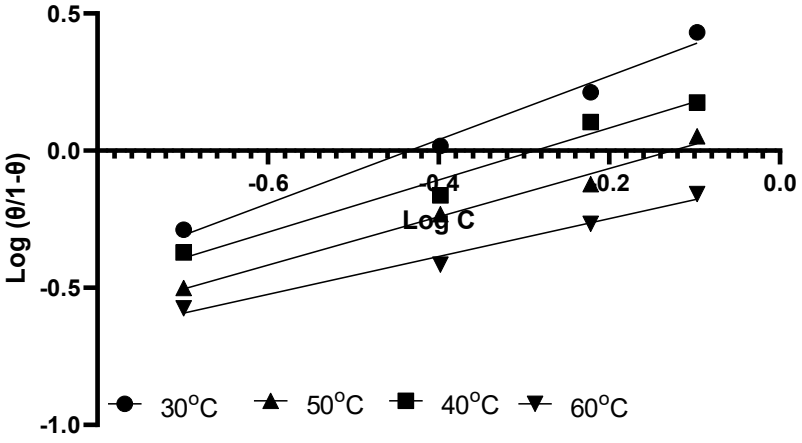

Fig. 8. El-Awady adsorption model values for mild steel in 1M H_2SO_4 and 0.2-0.8 g/L PRFSS concentration at 30, 40, 50, and 60°C

3.7.4. Equilibrium constant of adsorption (K_{ads}) and Gibbs free energy (ΔG_{ads})

The thermodynamic-kinetic equilibrium constant of adsorption (K_{ads}) measures the effectiveness of the adsorption interaction between the PRFSS inhibitor adsorbent molecule and the adsorbate (TABLE 6). The decrease in equilibrium constant of adsorption (K_{ads}) with increasing temperature suggests that the adsorption process is exothermic in nature. This means that the adsorption of PRFSS on the mild steel surface is more favorable at lower temperatures. The decrease in K_{ads} with increasing PRFSS concentration can be attributed to the saturation of the adsorption sites on the mild steel surface. At higher concentrations, there are more extract molecules competing for the same adsorption sites, resulting in a decrease in the number of molecules that are able to adsorb.

TABLE 6

Calculated values of K_{ads}, ΔG_{ads} (kJmol^{-1}) for mild steel dissolution in 1M H_2SO_4 and 0.2 g/L to 0.8 g/L PRFSS inhibitor concentration at 30°C, 40°C, 50°C and 60°C

Temperature (°C)	30	40	50	60
Equilibrium constant of adsorption (K_{ads})	0.6439	0.5357	0.3947	0.3322
Gibbs free energy of adsorption (ΔG_{ads}) (kJmol^{-1})	–8.02	–8.62	–9.50	–9.20

The decrease in Gibbs free energy of adsorption (ΔG_{ads}) with increasing temperature indicates that the adsorption process is spontaneous. The more negative the value of ΔG_{ads}, the more spontaneous the process. The decrease in ΔG_{ads} with increasing PRFSS concentration suggests that the adsorption process is more favorable at higher concentrations. This is because the higher the concentration of PRFSS, the more molecules there are available to adsorb on the mild steel surface, resulting in a greater decrease in ΔG_{ads}.

These results are consistent with those by Ebenso et al. [50] who found that the adsorption of *P. guajava* extract on mild steel in 0.5 M H_2SO_4 was exothermic and spontaneous. The decrease in K_{ads} and ΔG_{ads} with increasing temperature and inhibitor concentration were attributed to the saturation of the adsorption sites on the mild steel surface.

Another study by Oguzie et al. [51] found that the adsorption of *P. guajava* extract on mild steel in 1M H_2SO_4 was also exothermic and spontaneous. The decrease in K_{ads} and ΔG_{ads} with increasing temperature and inhibitor concentration were attributed to the formation of a protective layer on the mild steel surface. The decrease in K_{ads} and ΔG_{ads} with increasing temperature and PRFSS concentration in the inhibition of mild steel in 1M H_2SO_4 can be attributed to the exothermic nature of the adsorption process and the saturation of the adsorption sites on the mild steel surface.

3.7.5. Enthalpy of adsorption (Q_{ads}) and Activation energy (E_a)

TABLE 7 revealed an increase in enthalpy of adsorption (Q_{ads}) with increasing concentration of PRFSS which is likely due to the increased number of active sites on the extract surface that are available for interaction with the metal ions. The stronger interaction between PRFSS and the mild steel surface leads to a decrease in the activation energy (E_a) for the dissolution of mild steel. This is because the extract molecules act as a barrier between the mild steel surface and the corrosive species in the solution, which makes it more difficult for the mild steel to dissolve.

TABLE 7

Calculated values of activation energy (E_a) and heat of adsorption (Q_{ads}) for mild steel dissolution in 1M H_2SO_4 and 0.2 to 0.8 g/L PRFSS inhibitor concentration at 30°C and 60°C

PRFSS Concentration (g/L)	Blank	0.2	0.4	0.6	0.8
Activation energy (E_a)	45.73	50.08	55.84	60.49	66.92
Enthalpy of adsorption (Q_{ads})	—	–18.51	–26.42	–31.01	–38.01

The decrease in E_a with increasing PRFSS concentration has been reported by Abba-Aji et al. [59] found that the E_a for the dissolution of mild steel in 0.5M H_2SO_4 decreased from 75.8 kJ/mol to 58.9 kJ/mol with increasing concentration of *Vernonia amygdalina* extract.

The decrease in E_a with increasing inhibitor concentration can be explained by the fact that the inhibitor molecules compete with the corrosive species for adsorption sites on the metal surface. As the inhibitor concentration increases, the number of inhibitor molecules adsorbed on the surface increases, which decreases the number of sites available for the corrosive species. This leads to a decrease in the rate of dissolution and a decrease in the E_a.

3.8. Potentiodynamic Polarization Study

The polarization plot in Fig. 9 shows the relationship between the potential of a metal electrode and the current density flowing through it, which is a useful tool for studying the corrosion behaviour of metals. The polarization plot shows that the Tafel slopes of mild steel in 0.6 g/L, 0.2 g/L, 0.4 g/L and 0.8 g/L PRFSS inhibitor are 128.9 mV/decade, 109.8 mV/decade, 90.7 mV/decade and 78.6 mV/decade, respectively. Again, the Tafel slopes of mild steel in different concentrations of PRFSS inhibitor are close to each other, which indicates that the mechanism of corrosion inhibition of PRFSS inhibitor is the same at different concentrations.

The observed variations in the polarization curves with increasing PRFSS inhibitor concentrations suggest that the inhibitor is able to reduce the corrosion of the metal electrode in the acid medium. The higher the inhibitor concentration, the

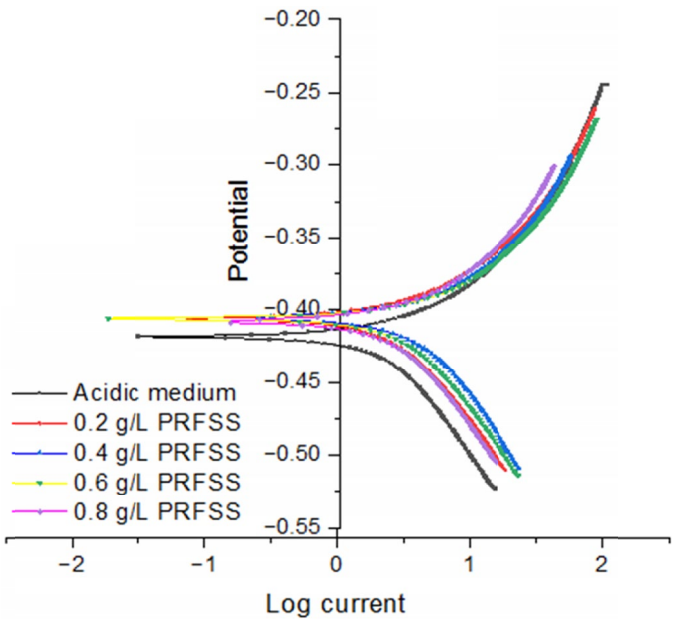

Fig. 9. Polarization plot of mild steel in an acidic medium and various PRFSS inhibitor concentration

more effective the inhibition, as seen by the progressive shift of the curves towards more positive potentials.

This indicates that the PRFSS inhibitor is capable of passivating the metal surface, reducing the anodic dissolution and/or cathodic oxygen reduction reactions that drive the corrosion process. The increased inhibition at higher concentrations implies that the inhibitor is adsorbing more strongly on the metal surface, forming a protective layer that hinders the corrosion reactions.

The observed inhibition behaviour aligns with findings reported by Obot et al. [60], which showed similar trends in the polarization curves for a corrosion inhibitor in an acidic environment, where higher inhibitor concentrations led to more effective corrosion mitigation. Another study by Singh et al. [61], also reported the enhanced inhibition performance of a compound at elevated concentrations in an acidic medium.

The potentiodynamic polarization parameters presented in TABLE 5 provide insights into the corrosion behaviour of mild steel in 1M H_2SO_4 solution with varying concentrations of the PFRSS inhibitor at 32°C.

The shift in E_{corr} towards more positive values indicates that the inhibitor is effective in suppressing the anodic dissolution of the metal. This further aligns with the findings reported by Obot et al. [60] where the authors observed a positive shift in E_{corr} for a corrosion inhibitor in an acidic environment. However, there was a decrease in I_{corr} with increasing inhibitor concentration suggesting that the PFRSS inhibitor is effective in reducing the corrosion rate of MSTC in the 1M H_2SO_4 solution. The corrosion current density of mild steel in acidic medium is 3.87E-05 A/cm^2, which is higher than that in 0.2 g/L (1.27E-05 A/cm^2), 0.4 g/L (0.89E-05 A/cm^2), 0.6 g/L (2.03E-05 A/cm^2), and 0.8 g/L (0.67E-05 A/cm^2) PRFSS inhibitor. This observation is consistent with the study by Singh et al. [60], where the authors reported enhanced inhibition performance of a compound at elevated concentrations in an acidic medium.

The decrease in β_a and β_c values with increasing inhibitor concentration indicates that the inhibitor is primarily affecting the anodic dissolution process because the influence but β_c values were affected to a lesser extent than the anodic reactions. Generally, there was an increase in %*IE* with increasing inhibitor concentration demonstrating the enhanced corrosion inhibition performance of the PFRSS inhibitor.

The observed trends in the potentiodynamic polarization parameters (E_{corr}, I_{corr}, β_a, β_c, and %*IE*) for MSTC corrosion in 1M H_2SO_4 with varying PFRSS inhibitor concentrations at 32°C are consistent with the findings reported in the literature, particularly the study of Odewunmi et al., [61] which showed that watermelon waste products was effective in reducing the corrosion rate of mild steel in HCl. The corrosion inhibition efficiency of PRFSS is likely due to the presence of polyphenols, which are known to be effective corrosion inhibitors. Polyphenolic compounds can form complexes with metal ions, which prevents them from reacting with oxygen and water to form corrosion products.

3.9. Characterisation of mild steel in 1M H_2SO_4 and PRFSS inhibitor

3.9.1. FT-IR analysis of mild steel after corrosion inhibition study

The spectra of the mild steel samples, Fig. 10, show peaks at 3853, 3729 and 3592 cm^{-1} can be attributed to O-H stretching of iron hydroxide from the iron oxide layer and adsorbed water,

TABLE 5

Calculated potentiodynamic polarization parameters and inhibition efficiency for mild steel corrosion in 1M H_2SO_4 and 0.2 to 0.8 g/L SSBT inhibitor concentration at 32°C

Inhibitor Conc. (g/L)	E_{corr} (mV vs SCE)	I_{corr} (mA/cm^2)	β_a (mV/dec)	β_c (mV/dec)	%*IE*
Blank	–418.45	414.46	133.19	–119.87	—
0.2	–407.15	287.94	81.41	–82.41	30.54
0.4	–404.20	239.06	69.97	–76.22	42.34
0.6	–404.76	109.70	72.05	–75.17	73.53
0.8	–407.81	85.81	67.64	–71.89	79.30

Keys: E_{corr} (mV vs SCE) – Corrosion Potential, I_{corr} (mA/cm^2) – Corrosion Current Density, β_a (mV/dec) – Anodic Tafel Slope, β_c (mV/dec) – Cathodic Tafel Slope, and %*IE* – Inhibition Efficiency.

the peaks around 2200 to 2000 cm^{-1} and 1700 to 1500 cm^{-1} can be attributed respectively to the C=O stretching and C-O stretching of carbon dioxide derivate species adsorbed at the surface of the samples [43,63,64].

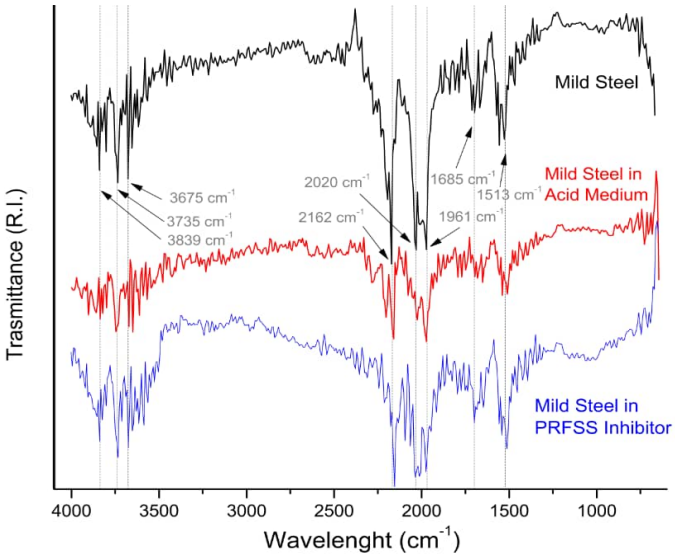

Fig. 10. FTIR spectrum of mild steel (black), mild steel in 1M H_2SO_4 (red), and mild steel in PRFSS inhibitor (blue)

Although, the samples present peaks at the same regions, the overall pattern of the spectra of the mild steel treated using PRFSS is different from the samples before and after corrosion process in 1M H_2SO_4, showing that the presence of the inhibitor modified the surface in a different way as the acid medium alone. This is consistent with the results of the potentiodynamic polarization curves, which showed that the PRFSS inhibitor interferes at the surface corrosion process.

3.9.2. Morphological analysis of MSTC after corrosion inhibition study

The SEM images in Fig. 11 provide a visual comparison of the surface morphology of mild steel under different conditions. In the blank medium the surface of the mild steel appears to be relatively smooth with visible linear striations. These striations are indicative of the mechanical finishing or polishing process the steel underwent. The surface shows minimal signs of corrosion or wear, implying a stable environment without aggressive chemical interactions. However, in 1M H_2SO_4 the surface is rough and extensively corroded, with a noticeable increase in pitting and irregularities compared to the blank medium. This rough and pitted surface is typical of the corrosive action of sulfuric acid, indicating substantial material degradation. The H_2SO_4 environment leads to aggressive corrosion, which is evidenced by the surface morphology showing significant damage (Fig. 11(b)). Comparatively, when Mild steel is placed in a PRFSS inhibitor in 1M H_2SO_4; the surface appears less rough and damaged compared to image (b) but not as smooth as image (a). There are fewer pits and the surface is more uniform. The PRFSS inhibitor has mitigated the corrosive effects of the sulfuric acid. The inhibitor forms a protective layer, reducing the acid's impact on the steel's surface. This leads to a comparatively smoother surface with fewer irregularities and decreased signs of corrosion.

The effects observed in the SEM images align well with documented studies by Abdulrahman et al. [65] who reported that well-polished steel surfaces in neutral environments show minimal signs of degradation, primarily dictated by mechanical finishing marks. However, according to Singh & Quraishi [66], the aggressive nature of sulfuric acid on mild steel is well-documented; literature describes significant pitting corrosion and surface roughening, which coincide with the observations in image (b). Furthermore, studies by El-Etre [67] and Umoren et al. [68] highlighted the effectiveness of plant based inhibitors in reducing the corrosion rate of steel in acidic environments. These inhibitors adsorb onto the steel's surface, forming a protective barrier that decreases the rate of corrosion. This is consistent with the reduced surface roughness and fewer pits seen in image (c).

4. Conclusion

The study on using a PRFSS as a corrosion inhibitor for mild steel in acidic environments yielded promising results. The

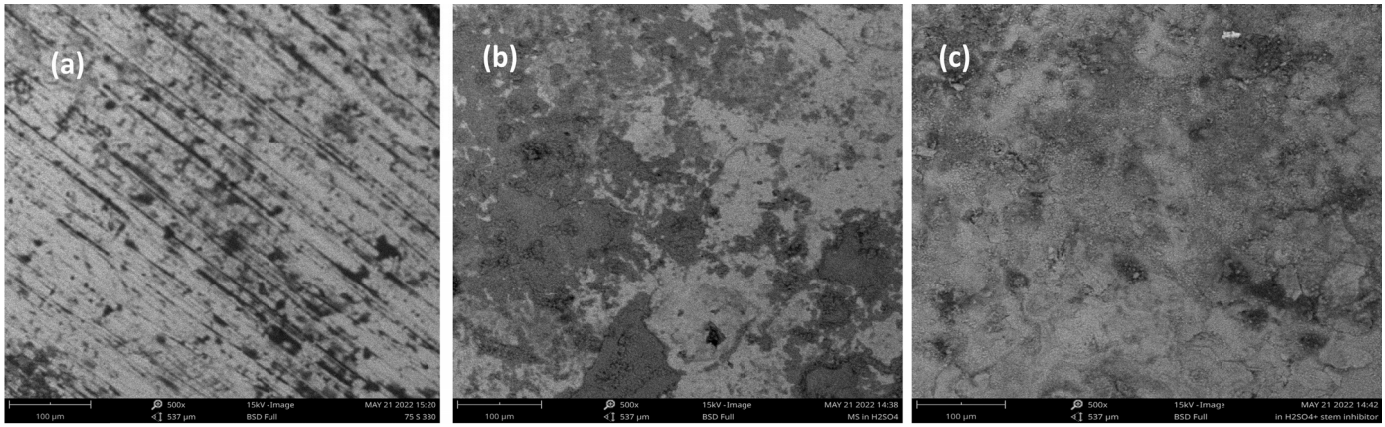

Fig. 11. Surface SEM images of mild steel in (a) blank medium (b) 1M H_2SO_4, and (c) 1M H_2SO_4 and PRFSS inhibitor at magnification ×500

extract, rich in tannins, phenols, and anthocyanins, effectively formed complexes with metal ions, preventing corrosion.

FTIR spectrum analysis confirmed the successful adsorption of the PRFSS inhibitor on the mild steel surface. The reduction in peaks further demonstrated the inhibitor's efficacy in forming a protective layer and mitigating interaction with corrodants. TGA showed two main stages of decomposition – moisture loss and organic matter decomposition – indicating thermal stability consistent with other plant-based extracts. Gravimetric measurements revealed a decrease in the corrosion rate of mild steel with higher concentrations of the PRFSS extract and an increase in surface coverage, suggesting that the polyphenolic compounds effectively formed a protective layer. It also showed substantive increase in corrosion rates as temperature increased. The adsorption behavior of PRFSS followed Langmuir, Freundlich, and El-Awady models, indicating a heterogeneous adsorption process. Thermodynamic parameters indicated that the process was exothermic and spontaneous, with stronger adsorption at lower temperatures. Polarization studies showed a positive shift in corrosion potential and a decrease in corrosion current density with higher concentrations of the PRFSS inhibitor, reducing anodic dissolution and oxygen reduction. SEM images revealed a smoother surface with fewer pits on mild steel treated with the PRFSS inhibitor compared to the significantly corroded surface exposed to sulfuric acid. This supports the protective role of the inhibitor.

The experimental findings validate the effectiveness of the PRFSS extract as a viable and environmentally friendly alternative to traditional chemical inhibitors, suggesting potential industrial applications in sectors like oil and gas, automotive, and construction. Future research could explore the long-term stability and performance of this green inhibitor under various conditions.

Funding

This research received no external financial support for the publication of this work.

Data Availability Statement

The data used to support this study are available within the manuscript.

Acknowledgments

The authors greatly acknowledge the University central laboratory, Umaru Musa Yaradua University Katsina, PMB2218 (www.umyu.edu.ng) Katsina State, Nigeria and the Faculty of Engineering, Ahmadu Bello University Zaria, Nigeria for their discipline of excellence for performing the analyses for the research.

REFERENCES

[1] N. Gayakwad, V. Patil, B.M. Rao, G.M. Gokale, K. Gurlhosur, Studies on Rhoeo discolor plant extract as a natural corrosion inhibitor. J. Environ. Eng. Sci. **16** (2), 66-76 (2021). DOI: https://doi.org/10.1680/jenes.20.00008

[2] E. Pagounis, M.J. Szczerba, R. Chulist, M. Laufenberg,Large Magnetic Field-Induced Work output in a NiMgGa Seven-Lavered Modulated Martensite. Appl. Phys. Lett. **107**, 152407 (2015). DOI: https://doi.org/10.1063/1.4933303

[3] C.B. Adindu, E.E. Oguzie, M.A. Chidiebere, Corrosion Inhibition and Adsorption Behavior of Extract of *Funtumia elastica* on Mild Steel in Acidic Solution. Int. Lett. Chem. Phys. Astron. **66**, 119-132 (2016). DOI: https://doi.org/10.18052/www.scipress.com/ilcpa.66.119

[4] N. Patni, S. Agarwal, P. Shah, Greener Approach towards Corrosion Inhibition. Chinese J. Eng. **2013**, 1-10 (2013). DOI: https://doi.org/10.1155/2013/784186

[5] R.S. Dubey, Green Corrosion Inhibitos Formetals and Alloys: a Comprehensive Review. Int. J. Adv. Res. **8**, (6), 1558-1565 (2020). DOI: https://doi.org/10.21474/ijar01/11247

[6] E.E. Oguzie, C.K. Enenebeaku, C.O. Akalezi, S.C. Okoro, A.A. Ayuk, E.N. Ejike, Adsorption and corrosion-inhibiting effect of Dacryodis edulis extract on low-carbon-steel corrosion in acidic media. J. Colloid Interf. Sci. **349** (1), 283-292 (2010). DOI: https://doi.org/10.1016/j.jcis.2010.05.027

[7] V. Rajeswari, D. Kesavan, M. Gopiraman, P. Viswanathamurthi, K. Poonkuzhali, T. Palvannan, Corrosion inhibition of Eleusine aegyptiaca and Croton rottleri leaf extracts on cast iron surface in 1 M HCl medium. Appl. Surf. Sci. **314**, 537–545 (2014). DOI: https://doi.org/10.1016/j.apsusc.2014.07.017

[8] J.H. Agresor, K.M.R. Cui-lim, Nypa fruticans (NIPA) starch filled with zinc oxide nanoparticles as corrosion inhibitor in steel. Mat. Sci., Chem. **54** (273), (2018).

[9] D. Atadious, N. Ogie, Controlling Induced-Corrosion in Oil pipelines: Determining the Inhibition Efficiency of Vernomiaamygdalina as a Natural Corrosion Inhibitor in comparison to Potassium Chromate. Scholarly J. Eng. Res. **4** (8), 25-30 (2021).

[10] L.T. Popoola, Progress on pharmaceutical drugs, plant extracts and ionic liquids as corrosion inhibitors. Heliyon. **5** (2), 1143 (2019). DOI: https://doi.org/10.1016/j.heliyon.2019.e01143

[11] P. A. Schweitzer (Ed.), Corrosion inhibitors, Corrosion and Corrosion Protection Handbook, 2nd Ed., Routledge, New York (2017).

[12] B.E.A. Rani, B.B.J. Basu, Green inhibitors for corrosion protection of metals and alloys: An overview. Int. J. Corros. **2012** (1), (2012). DOI: https://doi.org/10.1155/2012/380217

[13] S. Marzorati, L. Verotta, S.P. Trasatti, Green corrosion inhibitors from natural sources and biomass wastes. Molecules. **24** (1), (2019). DOI: https://doi.org/10.3390/molecules24010048

[14] J.C. Da Rocha, J.A. Da Cunha Ponciano Gomes, E. D'Elia, Aqueous extracts of mango and orange peel as green inhibitors for carbon steel in hydrochloric acid solution. Mater. Res. **17** (6), 1581-1587 (2014). DOI: https://doi.org/10.1590/1516-1439.285014

[15] H. Kaco et al., Enhanced corrosion inhibition using purified tannin in HCL medium. Malays. J. Anal. Sci. **22** (6), 931-942 (2018). DOI: https://doi.org/10.17576/mjas-2018-2206-02

[16] S.A. Umoren, U.M. Eduok, M.M. Solomon, A.P. Udoh, Corrosion inhibition by leaves and stem extracts of Sida acuta for mild steel in 1 M H2SO4 solutions investigated by chemical and spectroscopic techniques. Arab. J. Chem. **9**, S209-S224 (2016). DOI: https://doi.org/10.1016/j.arabjc.2011.03.008

[17] A. Abdulmajid, T.S. Hamidon, A.A. Rahim, M.H. Hussin, Tamarind shell tannin extracts as green corrosion inhibitors of mild steel in hydrochloric acid medium Mater. Res. Express. **6** (10), (2019). DOI: https://doi.org/10.1088/2053-1591/ab3b87

[18] Y. Yetri, Gunawarman, Emriadi, N. Jamarun, Theobroma cacao Peel Extract as the Eco-Friendly Corrosion Inhibitor for Mild Steel. Corros. Inhib. Princ. Recent Appl. InTech. (2018). DOI: https://doi.org/10.5772/intechopen.73263

[19] I. Eldin, H. Elgailani, C.Y. Ishak, Methods for Extraction and Characterization of Tannins from Some Acacia Species of Sudan. Pak. J. Anal. Environ. Chem. **17** (1), 43-49 (2016). DOI: https://doi.org/10.21743/pjaec/2016.06.007

[20] K.O. Omokhafe, Morphological Study of Acacia senegal (L.) Willd. from Borno and Yobe States, Nigeria. Int. J. Sci. & Eng. Res. **5** (8), 237-239 (2014).

[21] B. Anand, V. Balasubramanian, Corrosion behaviour of mild steel in acidic medium in presence of aqueous extract of Allamanda blanchetii. E-J. Chem. **8** (1), 226-230 (2011). DOI: https://doi.org/10.1155/2011/345095

[22] M.G. Sethuraman, P.B. Raja, Corrosion inhibition of mild steel by Datura metel in acidic medium. Pigm. Resin Technol. **34** (6), 327-331 (2005). DOI: https://doi.org/10.1108/03699420510630345

[23] P.B. Raja, M.G. Sethuraman, Natural products as corrosion inhibitor for metals in corrosive media – A review. Mater. Lett. **62** (1), 113-116 (2008). DOI: https://doi.org/10.1016/j.matlet.2007.04.079

[24] P.C. Okafor, M.E. Ikpi, I.E. Uwah, E.E. Ebenso, U.J. Ekpe, S.A. Umoren, Inhibitory action of Phyllanthus amarus extracts on the corrosion of mild steel in acidic media. Corros. Sci. **50** (8), 2310-2317 (2008). DOI: https://doi.org/10.1016/j.corsci.2008.05.009

[25] U. Garg, V. Kumpawat, R. Chauhan, R.K. Tak, Corrosion inhibition of copper by natural occurring plant Acacia senegal, J. Indian Chem. Soc. **88** (4), 513-519 (2011).

[26] P.J. Boden, Corrosion and corrosion control. Brit. Corros. J. **21** (3), 147 (1986). DOI: https://doi.org/10.1179/000705986798272190

[27] F. Bentiss, M. Traisnel, M. Lagrenee, The substituted 1,3,4-oxadiazoles: A new class of corrosion inhibitors of mild steel in acidic media. Corros. Sci. **42** (1), 127-146 (2000). DOI: https://doi.org/10.1016/S0010-938X(99)00049-9

[28] O. Benali, H. Benmehdi, O. Hasnaoui, C. Selles, R. Salghi, Green corrosion inhibitor: Inhibitive action of tannin extract of Chamaerops humilis plant for the corrosion of mild steel in 0.5M H2SO4. J. Mater. Environ. Sci. **4** (1), 127-138 (2013).

[29] K.S. Banu L. Cathrine, General Techniques Involved in Phytochemical Analysis. Int. J. Adv. Res. Chem. Sci. **2** (4), 25-32 (2015), [Online]. Available: www.arcjournals.org

[30] M. Wadhai, D. Ayate, V. Ujjainkar, Estimation of tannin content in leaves, bark and fruits of *Terminalia arjuna* Roxb. Int. J. Farm Sci. **9** (1), 61 (2019). DOI: https://doi.org/10.5958/2250-0499.2019.00004.1

[31] M.S. Rukaiyat, G.S. Abubakar, M.K. Fatima, Corrosion inhibition of mild steel using alkaloids and tannins extracts of *Jatropha curcas* in acidic media. Bayero J. Pure Appl. Sci. **10** (1), 311 (2018). DOI: https://doi.org/10.4314/bajopas.v10i1.62s

[32] N.A.A. Talib, S. Zakaria, C.C. Hua, N.K. Othman, Tannin bark melalauca cajuputi powell (Gelam) as green corrosion inhibitor of mild steel. AIP Conf. Proc. **1614** (2), 171-177 (2014). DOI: https://doi.org/10.1063/1.4895191

[33] I.A. Adejoro, F.K. Ojo, S.K. Obafemi, Corrosion inhibition potentials of ampicillin for mild steel in hydrochloric acid solution. J. Taibah Univ. Sci. **9** (2), 196-202 (2015). DOI: https://doi.org/10.1016/j.jtusci.2014.10.002

[34] C.C. Aralu, H.O. Chukwuemeka-Okorie, K.G. Akpomie, Inhibition and adsorption potentials of mild steel corrosion using methanol extract of Gongronema latifoliuim. Appl. Water Sci. **11** (2), 1-7 (2021). DOI: https://doi.org/10.1007/s13201-020-01351-8

[35] R.S. Peres, E. Cassel, D.S. Azambuja, Black Wattle Tannin As Steel Corrosion Inhibitor. ISRN Corros. **2012**, 1-9 (2012). DOI: https://doi.org/10.5402/2012/937920

[36] A.M. Shah, A.A. Rahim, S. Yahya, P.B. Raja, S.A. Hamid, Acid corrosion inhibition of copper by mangrove tannin. Pigm. Resin. Technol. **40** (2), 118-122 (2011). DOI: https://doi.org/10.1108/03699421111113783

[37] D. Sow, Antioxidant and antimicrobial activities of polyphenols from Senegalia senegal stem bark. Ind. Crop. Prod. **61**, 438-447 (2014).

[38] E. Ebenso, A. Ibhadode, C. Akalezi, E.I.E. Ebenso, Inhibition of mild steel corrosion in acidic medium by the aqueous extract of Baphia nitida stem bark. Green Chem. Lett. Rev. **7** (2), 129-138 (2014).

[39] N.O. Eddy, A.O. Odiongenyi, Corrosion inhibition and adsorption properties of ethanol extract of ITHeinsia crinata/IT on mild steel in H2SO4. Pigm. Resin Technol. **39** (5), 288-295 (2010). DOI: https://doi.org/10.1108/03699421011076407

[40] M. Mobin, M.A. Khan, M. Parveen, Inhibition of mild steel corrosion in acidic medium using starch and surfactants additives. J. Appl. Polym. Sci. **121**, (3), 1558-1565 (2011). DOI: https://doi.org/10.1002/app.33714

[41] B. Ndiwe et al., Desorption Behavior and Thermogravimetric Analysis of Bio-Hardeners. J. Renew. Mater. **10** (8), 2015-2027 (2022). DOI: https://doi.org/10.32604/jrm.2022.019891

[42] M.A. Pantoja-Castroa, H. González-Rodrígueza, Study by infrared spectroscopy and thermogravimetric analysis of Tannins and Tannic acid,. Rev. Latinoam. Química. **39** (3), 107-112 (2011).

[43] S.R.R. Marques, T.K.B. Azevêdo, A.R.F. de Castilho, R.M. Braga, A.S. Pimenta, Extraction, quantification, and ftir characterization

of bark tannins of four forest species grown in northeast brazil. Rev. Arvore. **45**, 1-10 (2021).
DOI: https://doi.org/10.1590/1806-908820210000041

[44] I.C.C.M. Porto, T.G. Nascimento, J.M.S. Oliveira, P.H. Freitas, A. Haimeur, R. França, Use of polyphenols as a strategy to prevent bond degradation in the dentin-resin interface. Eur. J. Oral Sci. **126** (2), 146-158 (2018).
DOI: https://doi.org/10.1111/eos.12403

[45] A. Saxena, A. Mishra, Study on the Effect of Trace Elements Additives on Mechanical Properties and Microstructure of Mild Steel. J. Mater. Eng. Performance **28** (12), 7341-7350 (2019).

[46] M. Torabian, M. Saremi, H. Idris, M. Gupta, Experimental investigation of corrosion behaviors of mild steel bilayered nanocomposite coatings. Trans. IMF **98** (6), 309-318 (2020).

[47] D. Zhang, Y. Li, X. Li, Q. Wang, Effect of Silicon on Secondary Phase Precipitation and Mechanical Properties in Low Alloy Steels. Mater. Sci. Forum **928**, 83-88 (2018).

[48] D.R. Gaskell, Introduction to the Thermodynamics of Materials. 5th Ed., Cambridge University Press, Boca Raton (2012).

[49] R. Imanishi, Y. Kaneko, K. Takahashi, T. Yamamoto, Effect of Cobalt Addition on High-Temperature Mechanical Properties of High-Mn Austenitic Steels. Metals. **7** (7), 268 (2017).

[50] E.E. Ebenso, N.O. Eddy, A.O. Odiongenyi, Inhibition of mild steel corrosion in 0.5MH2SO4 solution by extract of Pressium guajava. Port. Electrochim. Acta. **26** (2), 141-152 (2008).

[51] E.E. Oguzie, E.E. Ebenso, G.N. Onuoha, A.I. Onuchukwu, Effect of Pressium guajava extract on the corrosion inhibition of mild steel in H2SO4. J. Mater. Environ. Sci. **1** (2), 71-82 (2009).

[52] P.C. Okafor, E.E. Ebenso, U.J. Ekpe, Green approach to corrosion inhibition of mild steel in HCl and H2SO4 solutions by the leaf extracts of Pressium guajava. Green Chem. Lett. Rev. **3** (4), 257-265 (2010).

[53] S.A. Umoren, U.M. Eduok, M.M. Solomon, The effects of Pressium guajava leaf extracts on the corrosion inhibition of mild steel in acidic media. J. Mater. Environ. Sci. **1** (1), 43-54 (2010).

[54] V. Konovalova, The effect of temperature on the corrosion rate of iron-carbon alloys. Mater. Today Proc. **38**, 1326-1329 (2021).
DOI: https://doi.org/10.1016/j.matpr.2020.08.094

[55] H. Jouhari, H. Ajmani, Y. Mouzdahir, Adsorption of Senegalia senegal extract onto copper: A mechanistic study. J. Environ. Chem. Eng. **8** (6), 104570 (2020).

[56] H. Jouhari, H. Ajmani, Y. Mouzdahir, Adsorption of Senegalia senegal extract onto aluminum: Equilibrium, kinetic and thermodynamic studies J. Taiwan Inst. Chem. Eng. **135**, 104372 (2023).

[57] M.Y. El-Awady, S.S. Al-Deyab, N.I. El-Agamy, Adsorption characteristic of methylene blue onto activated carbon. Int. J. Environ. Sci. Technol. **5** (2), 205-212 (2008).

[58] M.I. El-Khaiary, A.M. Yehia, H. El-Saied, Adsorption of phenol onto silica gel surfaces: Modeling, kinetics, and diffusion. J. Dispers. Sci. Technol. **31** (8), 1114-1132 (2010).

[59] M.A. Abba-Aji, A.B. Muhammad, D.D. Onwe, Corrosion inhibition of mild steel determined using blended bitter leaf extract and honey in dilute H2SO4 and HCl solutions. Arid Zo. J. Eng. Technol. Environ. **16** (4), 763-772 (2020).

[60] I.B. Obot, N.O. Obi-Egbedi, S.A. Umoren, Adsorption characteristics and corrosion inhibitive properties of clotrimazole for aluminium corrosion in hydrochloric acid. Int. J. Electrochem. Sc. **4** (6), 863-877 (2009).
DOI: https://doi.org/10.1016/s1452-3981(23)15190-x

[61] A. Singh, I. Ahamad, D.K. Yadav, V.K. Singh, M.A. Quraishi, The effect of environmentally benign fruit extract of Shahjan (Moringa oleifera) on the corrosion of mild steel in hydrochloric acid solution. Chem. Eng. Commun. **199** (1), 63-77 (2012).
DOI: https://doi.org/10.1080/00986445.2011.570390

[62] N.A. Odewunmi, S.A. Umoren, Z.M. Gasem, Watermelon waste products as green corrosion inhibitors for mild steel in HCl solution. J. Environ. Chem. Eng. **3** (1), 286-296 (2015).
DOI: https://doi.org/10.1016/j.jece.2014.10.014

[63] G. Socrates, Infrared and Raman characteristic group frequencies. Tables and charts, (3rd ed.), John Wiley & Sons, Inc. (2001).

[64] M.P. Castro, H.G. Rodriguez, Study by infrared spectroscopy and thermogravimetric analysis of Tannins and Tannic acid. Rev. Latinoam. Química. **39** (3), 107-112 (2011).

[65] A.S. Abdulrahman, M. Ismail, M.S. Hussain, Corrosion inhibitors for steel reinforcement in concrete: A review. Sci. Res. Essays. **6** (20), 4152-4162 (2011).
DOI: https://doi.org/10.5897/SRE11.1051

[66] A.K. Singh, M.A. Quraishi, The effect of some bis-thiadiazole derivatives on the corrosion of mild steel in hydrochloric acid. Corros. Sci. **52** (4), 1373-1385 (2010).
DOI: https://doi.org/10.1016/j.corsci.2010.01.007

[67] A.Y. El-Etre, Inhibition of aluminum corrosion using Opuntia extract. Corros. Sci. **45** (11), 2485-2495 (2003).
DOI: https://doi.org/10.1016/S0010-938X(03)00066-0

[68] S.A. Umoren, O. Ogbobe, I.O. Igwe, E.E. Ebenso, Inhibition of mild steel corrosion in acidic medium using synthetic and naturally occurring polymers and synergistic halide additives. Corros. Sci. **50** (7), 1998-2006 (2008).
DOI: https://doi.org/10.1016/j.corsci.2008.04.015